

## Two-dimensional $p$ -wave superconducting states with magnetic moments on a conventional $s$ -wave superconductor

Sho Nakosai,<sup>1</sup> Yukio Tanaka,<sup>2</sup> and Naoto Nagaosa<sup>3,1</sup>

<sup>1</sup>*Department of Applied Physics, University of Tokyo, Tokyo 113-8656, Japan*

<sup>2</sup>*Department of Applied Physics, Nagoya University, Aichi 464-8603, Japan*

<sup>3</sup>*RIKEN Center for Emergent Matter Science (CEMS), Wako 351-0198, Japan*

(Received 16 June 2013; published 6 November 2013)

Unconventional superconductivity induced by the magnetic moments in a conventional spin-singlet  $s$ -wave superconductor is theoretically studied. By choosing the spin directions of these moments, one can design spinless pairing states appearing within the  $s$ -wave superconducting energy gap. It is found that the helix spins produce a  $p_x + p_y$ -wave state while the skyrmion crystal configuration a  $p_x + ip_y$ -wave-like state. Nodes in the energy gap and the zero-energy flat band of Majorana edge states exist in the former case, while the chiral Majorana channels along edges of the sample and the zero-energy Majorana bound state at the core of the vortex appear in the latter case.

DOI: [10.1103/PhysRevB.88.180503](https://doi.org/10.1103/PhysRevB.88.180503)

PACS number(s): 74.45.+c, 74.20.-z, 74.78.-w

*Introduction.* Unconventional superconducting states are one of the most important issues in current condensed matter physics.<sup>1-3</sup> Although most of the superconductors show the conventional spin-singlet  $s$ -wave pairing, strongly correlated materials sometimes show unconventional pairing since the on-site pairing is suppressed by the repulsive interaction. However, the discovery of the unconventional pairings relies on serendipity to some degree, and their theoretical designs and artificial fabrications are highly desired. Especially, recent intensive interest in the topological superconductivity and consequent Majorana fermions enhance the importance of this topic since Majorana fermions are the leading candidate for the platform of quantum computation.<sup>4-9</sup>

A promising proposal for realization of a topological superconducting state is the combined system of a semiconducting nanowire with an  $s$ -wave superconductor under an external magnetic field. The spin-orbit interaction and the magnetic field reduce the degrees of freedom of electrons concerning superconducting states, and effectively generate a spinless  $p$ -wave superconductor.<sup>10-14</sup> As for one-dimensional systems, signals suggesting Majorana fermions at the ends of the nanowire have been observed in some experimental setups.<sup>15-18</sup> There are other routes for creating topological superconductors: a spin-singlet superconductor deposited on the topological insulator,<sup>19,20</sup> a superfluid of cold atoms with laser-generated effective spin-orbit interaction,<sup>21</sup> aligned quantum dots connected by  $s$ -wave superconductors,<sup>22</sup> and magnetic moments in  $s$ -wave superconductors<sup>23-26</sup> or nodal superconductors.<sup>27</sup> The last ones are significantly distinct in that they do not explicitly require spin-orbit interaction in the system. With respect to the cooperation between magnetic moment and superconductivity, it has been known that the bound states are created around the impurities with the energy inside the bulk superconducting gap (not necessarily zero energy).<sup>28-30</sup> The modulation of the local density of states by a single magnetic impurity has been observed in experiment.<sup>31</sup> The authors of Refs. 24 and 26 considered a one-dimensional array of magnetic impurities, and studied the possibility of the Kitaev state with the Majorana bound states at the ends of the array. The influence of magnetic moments on a superconductor

by the proximity effect has been intensively studied albeit in different interests.<sup>32-34</sup> On the other hand, it has been recognized that the spin-orbit interaction at the interface results in Rashba-type interaction and hence noncollinear spin configuration is organized.<sup>35</sup> Especially, the skyrmion crystal state is observed at the interface of Fe and Ir.<sup>36</sup> Therefore, the magnetic proximity effect of noncollinear moments to a superconductor becomes a realistic and important issue.

In this Rapid Communication, we propose a generic principle to design unconventional superconductivity in terms of noncollinear/noncoplanar configurations of magnetic moments on the surface of an  $s$ -wave superconductor. We derive an effective model constituted from the bound states around magnetic moments. The effective pair potentials as well as transfer integrals in the effective model depend on the directions of two neighboring moments. We show that a  $p_x + p_y$ -wave pairing state with nodes in the energy gap is generated by a noncollinear helical spin configuration, and moreover, we design a topological  $p_x + ip_y$ -wave-like state by means of a noncoplanar skyrmion crystal configuration of moments, as evidenced by chiral Majorana channels along the edges of the system and zero-energy Majorana bound states at the cores of vortices.

*Model.* Figure 1(a) shows a schematic illustration of the present model. We analyze the following tight-binding Hamiltonian describing a double-exchange model with the superconducting order parameter defined on a square lattice:

$$H = - \sum_{(ij)\sigma} t c_{i\sigma}^\dagger c_{j\sigma} - \sum_i \mu c_{i\sigma}^\dagger c_{i\sigma} + \sum_i \Delta_0 (c_{i\uparrow}^\dagger c_{i\downarrow}^\dagger + \text{H.c.}) - \sum_i J \mathbf{S}_i \cdot \boldsymbol{\sigma}_{\alpha\beta} c_{i\alpha}^\dagger c_{i\beta}. \quad (1)$$

The first three terms describe a conventional spin-singlet  $s$ -wave superconductor with the transfer integral  $t$ , the chemical potential  $\mu$ , and the pairing potential  $\Delta_0$ . In addition, electrons couple with magnetic moments located at sites  $i$  with the strength  $J$  through the double-exchange mechanism. This model can describe the interface between a bulk  $s$ -wave superconductor and a magnetic material. We assume that

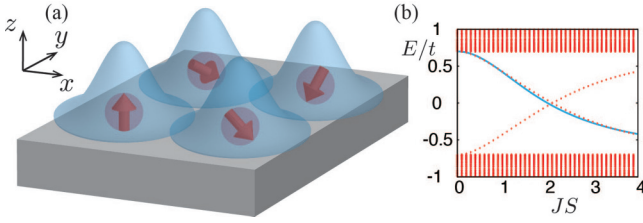


FIG. 1. (Color online) (a) Schematic illustration for the formation of an effective lattice model from the bound states localized around magnetic moments on the surface of an  $s$ -wave superconductor [see Eq. (3)]. (b) Energy levels of quasiparticles obtained by a tight binding model calculation with a single moment with  $\Delta_0/t = 0.7$  in Eq. (1).  $J$  is the coupling constant between electrons and magnetic moment and  $S$  is the magnitude of the spin moment. The solid (blue) curve shows the analytical solution  $E_0$  for the continuum model (see the main text).

the pairing potential is not affected by magnetic moments, which are supposed to be solidly ordered. Below we construct unconventional superconducting states with some particular structures of magnetic moments. We derive an effective model in the aim of choosing appropriate magnetic order for intended unconventional states before directly solving Eq. (1). First, we start with the case of a single moment in a superconductor. The Bogoliubov–de Gennes equations are given by

$$\begin{aligned} (\xi_k - E)u_{k\uparrow} - \frac{JS}{V} \sum_l u_{l\uparrow} + \Delta_0 v_{k\downarrow} &= 0, \\ (\xi_k + E)v_{k\downarrow} + \frac{JS}{V} \sum_l v_{l\downarrow} - \Delta_0 u_{k\uparrow} &= 0, \end{aligned} \quad (2)$$

where we set the origin at the site of moment,  $\hbar = 1$ , and  $\xi(\mathbf{k}) = -2t(\cos k_x + \cos k_y) - \mu$  is the tight-binding dispersion. The numerical result of the energy level is shown in Fig. 1(b). The dispersion can be approximated in the continuum limit as  $\xi(\mathbf{k}) = \frac{k^2}{2m} - \mu - 4t$  with  $m = (2t)^{-1}$ . We can find solutions with energy  $\pm E_0 = \pm \Delta_0 [1 - (\pi JS N_0/2)^2] / [1 + (\pi JS N_0/2)^2]$ , where  $N_0$  is the density of states in the normal phase<sup>28–30,38</sup> [solid line in Fig. 1(b)]. With increasing the magnitude of  $JS$ ,  $E_0$  changes from  $\Delta_0$  to  $-\Delta_0$  within the bulk superconducting energy gap. The corresponding wave functions are real and asymptotically given for  $r \rightarrow \infty$  as

$$\begin{aligned} u_{\uparrow}(\mathbf{r}) &\sim \frac{\sin(p_F r - \delta_+)}{p_F r} \exp\left[-\frac{r}{\xi_0} |\sin(\delta_+ - \delta_-)|\right], \\ v_{\downarrow}(\mathbf{r}) &\sim \frac{\sin(p_F r - \delta_-)}{p_F r} \exp\left[-\frac{r}{\xi_0} |\sin(\delta_+ - \delta_-)|\right], \end{aligned} \quad (3)$$

where we define some quantities:  $\tan \delta_{\pm} = \pm \pi JS N_0/2$ ,  $p_F$  is the Fermi momentum,  $v_F = p_F/m$  is the Fermi velocity, and  $\xi_0 = v_F/(\pi \Delta)$ . When the moments are aligned in a lattice, we expect that the bound state around each moment has overlap with neighboring bound states. The overlap causes effective transfer integrals and pair potentials among the bound states. The low-energy properties, i.e., in the bulk superconducting gap, can be described by an effective BdG lattice model constructed from these bound states. One can find similar arguments in Refs. 24–26.

*Design of  $p$ -wave superconducting states.* We propose a principle to design the superconducting states appearing within the gap of the host spin-singlet  $s$ -wave superconductor. It will be shown that configurations of magnetic moments play the essential role for the emergence of unconventional superconducting states. In the previous section, we assumed the magnetic moment parallel to the  $+s_z$  direction. Here, we introduce a unitary transformation for the description of general directions of moments. The coupling term with magnetic moments in Eq. (1) can be transformed as

$$\psi_{\alpha}^{\dagger} \mathbf{S} \cdot \boldsymbol{\sigma}_{\alpha\beta} \psi_{\beta} = (U \psi)^{\dagger} U \mathbf{S} \cdot \boldsymbol{\sigma} U^{\dagger} U \psi = \tilde{\psi}^{\dagger} S \sigma_z \tilde{\psi} \quad (4)$$

by the unitary matrix

$$U^{\dagger} = \begin{pmatrix} \cos \frac{\theta}{2} & -e^{-i\phi} \sin \frac{\theta}{2} \\ e^{i\phi} \sin \frac{\theta}{2} & \cos \frac{\theta}{2} \end{pmatrix}, \quad (5)$$

where  $\theta$  and  $\phi$  are the polar coordinates such that  $\mathbf{S} = S(\sin \theta \cos \phi, \sin \theta \sin \phi, \cos \theta)$ . The wave functions for arbitrary spin directions are obtained by operating  $U^{\dagger}$  on Eqs. (3). Then, the electron operators are expressed for the low-energy sector as

$$\begin{aligned} \psi_{\uparrow} &= \sum_i \left[ \cos \frac{\theta_i}{2} u_{\uparrow}(\mathbf{r} - \mathbf{r}_i) \alpha_i - e^{-i\phi_i} \sin \frac{\theta_i}{2} v_{\downarrow}^*(\mathbf{r} - \mathbf{r}_i) \alpha_i^{\dagger} \right], \\ \psi_{\downarrow} &= \sum_i \left[ e^{i\phi_i} \sin \frac{\theta_i}{2} u_{\uparrow}(\mathbf{r} - \mathbf{r}_i) \alpha_i + \cos \frac{\theta_i}{2} v_{\downarrow}^*(\mathbf{r} - \mathbf{r}_i) \alpha_i^{\dagger} \right], \end{aligned} \quad (6)$$

where  $\alpha_i$  is the annihilation operator of the bound state around the moment located at site  $i$ . By substituting Eqs. (6) into the original Hamiltonian Eq. (1), we obtain

$$H_{\text{eff}} = \sum_i E_0 \alpha_i^{\dagger} \alpha_i + \sum_{\langle ij \rangle} [\bar{t}_{ij} \alpha_i^{\dagger} \alpha_j + (\bar{\Delta}_{ij} \alpha_i^{\dagger} \alpha_j^{\dagger} + \text{H.c.})], \quad (7)$$

where  $\bar{t}_{ij}$  and  $\bar{\Delta}_{ij}$  are effective transfer integrals and pair potentials for the nearest neighbor sites  $\langle i, j \rangle$  in the present low-energy Hamiltonian. We keep them up to the nearest neighboring sites. Here, we define

$$\hat{z}_i = \begin{pmatrix} \cos \frac{\theta_i}{2} \\ e^{i\phi_i} \sin \frac{\theta_i}{2} \end{pmatrix}, \quad (8)$$

which represents the spin as  $\mathbf{S}_i = S \hat{z}_i^{\dagger} \boldsymbol{\sigma} \hat{z}_i$ . The effective transfer integrals and pair potentials are represented by

$$\bar{t}_{ij} = \hat{z}_i^{\dagger} \hat{z}_j \bar{t}_0, \quad (9)$$

$$\bar{\Delta}_{ij} = \hat{z}_i^{\dagger} i \sigma_y \hat{z}_j^* \bar{\Delta}_0, \quad (10)$$

with  $\bar{t}_0 = \int d\mathbf{r} \{ [u_i \xi(\mathbf{r}) u_j - v_i \xi(\mathbf{r}) v_j] + \Delta_0 (u_i u_j + v_i v_j) \}$ ,  $\bar{\Delta}_0 = \int d\mathbf{r} \{ [u_i \xi(\mathbf{r}) v_j + v_i \xi(\mathbf{r}) u_j] + \Delta_0 (u_i u_j - v_i v_j) \}$ ,  $u_i = u_{\uparrow}(\mathbf{r} - \mathbf{r}_i)$ , and  $v_i = v_{\downarrow}(\mathbf{r} - \mathbf{r}_i)$ . Based on these equations, we can design various kinds of superconducting states. Note that  $\bar{t}_{ij}$  and  $\bar{\Delta}_{ij}$  are invariant for the common rotation of both moments at sites  $i$  and  $j$ . Namely, these quantities depend only on the relative direction of the two moments. The electron spin of the bound state is uniquely determined by the magnetic moment, and hence we have a spinless lattice model with controllable parameters depending on the configuration of moments.

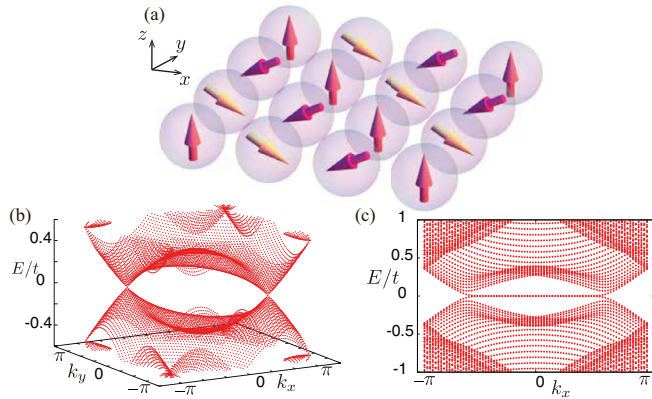


FIG. 2. (Color online) (a) Configuration of moments producing effective  $p_x + p_y$ -wave pairing. All spins lie in the  $s_x s_z$ -plane rotating by  $2\pi/3$  along both  $x$  and  $y$  directions; therefore a  $3 \times 3$  block constitutes a unit cell. (b) Energy spectrum of quasiparticles with the configuration in (a) calculated by the tight-binding model [Eq. (1)] with  $t = 1.0$  and  $\Delta_0 = 0.7$ . The spectrum has two point nodes as expected. (c) Energy spectrum with open boundaries. One can see dispersionless Andreev bound states connecting two nodal points.

*Numerical studies.* We design two-dimensional superconducting states by choosing appropriate configurations of moments designed from Eqs. (9) and (10) (see part A of the Supplemental Material<sup>37</sup>). We investigate properties of the system by directly solving the original tight-binding Hamiltonian [Eq. (1)]. The calculations are performed with transfer integral  $t = 1.0$  and on-site superconducting order parameter of the host conventional superconductor  $\Delta_0 = 0.7$ . The magnetic moment is attached to each site. We consider both periodic and open boundary conditions to see bulk properties and edge states of the system, respectively. Hereafter when we calculate the dispersion of Andreev bound states, we use a cylindrical configuration with open boundaries along the  $y$  direction. We consider the following two cases:  $p_x + p_y$ -wave pairing and  $p_x + ip_y$ -wave-like pairing.

(1) *Nodal superconductor.* We can see from Eqs. (9) and (10) that  $\bar{\Delta}_{ij}$  vanishes when the two neighboring moments point in the same direction ( $\theta_i = \theta_j, \phi_i = \phi_j$ ), while  $\bar{t}_{ij}$  vanishes for the opposite direction ( $\theta_i = \pi - \theta_j, \phi_i = \phi_j + \pi$ ). Therefore, noncollinear spin configurations are required to obtain the nontrivial states. We know that a one-dimensional helical or spiral spin structure generates  $p$ -wave superconducting states.<sup>26</sup> We can generalize this to two dimensions. We choose the spinor  $\hat{z}_i$ 's so that spins rotate by  $2\pi/3$  around the  $s_y$  axis along both the  $x$  and  $y$  directions as shown in Fig. 2(a) and Fig. S1 in the Supplemental Material;<sup>37</sup> all the moments lie in the  $s_x s_z$  plane. The resulting state is expected to have a real order parameter with  $p$ -wave pairing for the  $x$  and  $y$  directions. This can be named as the  $p_x + p_y$ -wave pairing state. The present superconducting state is not stabilized as a bulk phase because it is energetically disadvantageous compared with chiral  $p$ -wave pairing without nodal structures. However, in the model considered here, induced  $p$ -wave pairing is localized in the vicinity of the surface of the bulk superconductor and is controlled by the configuration of moments. As a result, the  $p_x + p_y$ -wave pairing state is realized by a single spiral

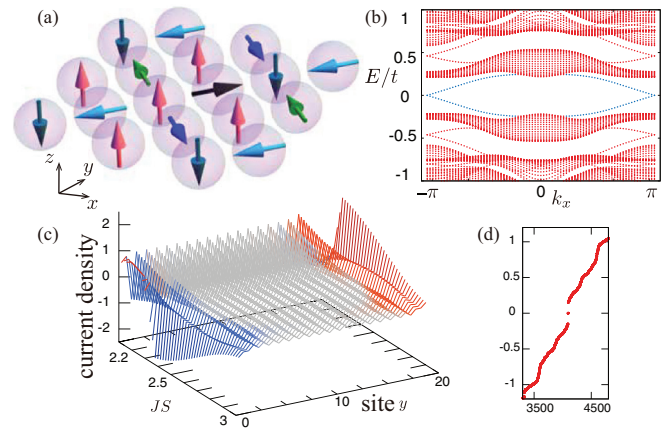


FIG. 3. (Color online) (a) Configuration of skyrmion lattice producing an effective fully gapped superconducting phase [see also Fig. S6 in the Supplemental Material (Ref. 37)]. (b) Energy spectrum of quasiparticles with the configuration in (a) calculated by the tight-binding model [Eq. (1)] with  $t = 1.0$  and  $\Delta_0 = 0.7$  with open boundary conditions along the  $y$  direction. One can see linearly dispersing bands at  $k_x = \pm\pi$  which are localized at the boundaries of the system. (c) Current density calculated with the configuration given in (a) with 20 unit cells along the  $y$  direction. One can see finite current density at the edges of the system, which is crucial evidence for a topologically nontrivial phase. (d) Energy levels of quasiparticles obtained by a tight binding model calculation with vortices. The horizontal axis shows the indices of energy eigenvalues. The system size is set  $16 \times 16$  with periodic boundary conditions, and  $t = \Delta_0 = 1.0$ . The zero-energy states are fourfold degenerate.

structure of moments. We have tested our expectation by numerical calculations solving Eq. (1). Figure 2(b) shows the dispersion of the quasiparticles, where the induced energy gap has nodes on the line of  $k_x = -k_y$ . We also calculate Andreev bound states at the boundary of the system. The resulting dispersions have flat bands, which are believed to be a hallmark of unconventional superconductors.<sup>39–42</sup> It is noted that flat bands of zero-energy bound states are realized starting from conventional  $s$ -wave superconducting pairing. One can find in Ref. 43 a related work.

(2) *Chiral  $p$ -wave superconductor.* Next we attempt to generate fully gapped superconducting states. For this purpose, the phase of pair potential along the  $x$  and  $y$  directions should be different. The case where the phase difference is equal to  $\pi/2$  is well known as a chiral  $p$ -wave superconductor. We can always choose the phases of the pairing order parameter  $\Delta_{ij}$  as real by appropriate gauge transformation once the moments lie in a plane. Then we need to consider noncoplanar spin configurations. Here we study the case of the skyrmion crystal state [Fig. 3(a)] recently observed experimentally.<sup>35,36</sup> In this case, moments obviously have a noncoplanar configuration. The parameters in the effective model calculated by Eqs. (9) and (10) are given in the Supplemental Material<sup>37</sup> (Fig. S2). We have confirmed the following properties of the system, and based on them we conclude that it has the same topological nature as chiral  $p$ -wave superconducting states while the transfer integrals and pair potentials are not uniform with this configuration. The characteristic properties of chiral  $p$ -wave superconductors are (i) the full gap nature, (ii) the existence

of edge modes and currents, and (iii) the emergence of zero-energy states at the cores of vortices.<sup>44</sup> First we have confirmed that the system has an energy gap in the whole Brillouin zone by the same calculation as Fig. 2(b), which indicates the complex value of the pair potential because the system is essentially spinless. Figure 3(b) shows the energy dispersion of quasiparticles with the open boundaries. One can see two linearly dispersing bands crossing at  $k_x = \pm\pi$ , which are localized at the edges of the system.<sup>45</sup> Here the Fermi surface in the normal state is hole-like; then chiral edge modes cross at  $k_x = \pm\pi$ , not  $k_x = 0$ . The fact that these modes yield edge current is manifested by directly calculating current density

$$j_i = \sum_{k_x, \sigma} 2t \sin k_x \alpha_{i\sigma}^\dagger(k_x) \alpha_{i\sigma}(k_x). \quad (11)$$

The result is shown in Fig. 3(c). At  $JS \sim 2.4$  the clear signal appears indicating the topological quantum phase transition. We also confirmed that zero-energy Majorana bound states appear at the cores of vortices [Fig. 3(d)]. We conclude that the resulting superconducting state is in the same topological phase as the chiral  $p$ -wave superconductor based on these observations. As another example of the noncoplanar spin configuration, we study the double-spiral structure in part B of the Supplemental Material<sup>37</sup> and find the similar  $p_x + ip_y$ -wave-like state.

*Discussion and conclusions.* In this Rapid Communication, we have proposed a new way of creating effective two-dimensional unconventional superconductivity by local moments on the conventional spin-singlet  $s$ -wave superconductor. The noncollinear configurations of moments are essential to induce  $p$ -wave pairing. There is a hierarchical structure in energy scale, i.e., the original  $s$ -wave energy gap and that of the induced  $p$ -wave superconductivity. Andreev bound states by a topological origin appear within the latter energy gap. Even the chiral  $p_x + ip_y$ -wave-like pairing is realized by the noncoplanar configuration of moments, which shows the chiral

Majorana edge channel with linear dispersion and zero-energy Majorana bound states at the vortex cores. Moreover it indicates that we can create various kinds of superconducting states by choosing appropriate configurations of moments. For example, by changing the distance between the moments, one can tune the magnitudes of effective transfer integrals and pair potentials. Then, the anisotropy  $|t_x/t_y|$  can be controlled to obtain the rich topological phases discussed in Ref. 46. Here we briefly discuss the effect of self-energy correction and spin fluctuation for legitimizing our approach and results. The self-energy correction due to the dynamical quantum fluctuation of spins can be estimated as  $\text{Re}\Sigma(\varepsilon) \sim \lambda\varepsilon$  and  $\text{Im}\Sigma(\varepsilon) \sim \lambda\varepsilon^2/\varepsilon_F$ , where  $\lambda = J^2S/(I\varepsilon_F)$  is the dimensionless coupling constant with  $I$  being the exchange coupling between spins in the magnet, and  $\varepsilon_F$  the Fermi energy of the superconductor. This correction is tiny at small electron energy  $\varepsilon$ , and does not change the minigap structure. Also we have confirmed numerically the robustness of the induced gap structure against the small (static) spin fluctuation as shown in Fig. S6 in the Supplemental Material.<sup>37</sup> Though our model will simulate the interface of bulk superconductors and magnetic materials, we end with an account of another experimental realization of these proposals. To create intended patterns of magnetic moments, we can use atomic manipulation techniques using scanning tunneling microscopy.<sup>47,48</sup> The spin structure in organized magnetic impurities is also observed,<sup>49,50</sup> although it is antiferromagnetic and cannot be utilized for our proposal.

*Acknowledgments.* S.N. was supported by a Grant-in-Aid for JSPS Fellows. This work was supported by a Grant-in-Aid for Scientific Research (S) (Grant No. 24224009); the Funding Program for World-Leading Innovative RD on Science and Technology (FIRST Program); the Strategic International Cooperative Program (Joint Research Type) from the Japan Science and Technology Agency; and Innovative Areas “Topological Quantum Phenomena” (Grant No. 22103005) from the Ministry of Education, Culture, Sports, Science, and Technology of Japan.

<sup>1</sup>M. Sigrist and K. Ueda, *Rev. Mod. Phys.* **63**, 239 (1991).

<sup>2</sup>F. Steglich, J. Aarts, C. D. Bredl, W. Lieke, D. Meschede, W. Franz, and H. Schäfer, *Phys. Rev. Lett.* **43**, 1892 (1979).

<sup>3</sup>Y. Tanaka, M. Sato, and N. Nagaosa, *J. Phys. Soc. Jpn.* **81**, 011013 (2012).

<sup>4</sup>N. Read and D. Green, *Phys. Rev. B* **61**, 10267 (2000).

<sup>5</sup>D. A. Ivanov, *Phys. Rev. Lett.* **86**, 268 (2001).

<sup>6</sup>G. Moore and N. Read, *Nucl. Phys. B* **360**, 362 (1991).

<sup>7</sup>C. Nayak, S. H. Simon, A. Stern, M. Freedman, and S. Das Sarma, *Rev. Mod. Phys.* **80**, 1083 (2008).

<sup>8</sup>X.-L. Qi and S.-C. Zhang, *Rev. Mod. Phys.* **83**, 1057 (2011).

<sup>9</sup>J. Alicea, *Rep. Prog. Phys.* **75**, 076501 (2012).

<sup>10</sup>J. D. Sau, R. M. Lutchyn, S. Tewari, and S. Das Sarma, *Phys. Rev. Lett.* **104**, 040502 (2010).

<sup>11</sup>J. Alicea, *Phys. Rev. B* **81**, 125318 (2010).

<sup>12</sup>R. M. Lutchyn, J. D. Sau, and S. Das Sarma, *Phys. Rev. Lett.* **105**, 077001 (2010).

<sup>13</sup>Y. Oreg, G. Refael, and F. von Oppen, *Phys. Rev. Lett.* **105**, 177002 (2010).

<sup>14</sup>T. D. Stanescu and S. Tewari, *J. Phys.: Condens. Matter* **25**, 233201 (2013).

<sup>15</sup>V. Mourik, K. Zuo, S. M. Frolov, S. R. Plissard, E. P. A. M. Bakkers, and L. P. Kouwenhoven, *Science* **336**, 1003 (2012).

<sup>16</sup>M. T. Deng, C. L. Yu, G. Y. Huang, M. Larsson, P. Caroff, and H. Q. Xu, *Nano Lett.* **12**, 6414 (2012).

<sup>17</sup>L. P. Rokhinson, X. Liu, and J. K. Furdyna, *Nat. Phys.* **8**, 795 (2012).

<sup>18</sup>A. Das, Y. Ronen, Y. Most, Y. Oreg, M. Heiblum, and H. Shtrikman, *Nat. Phys.* **8**, 887 (2012).

<sup>19</sup>L. Fu and C. L. Kane, *Phys. Rev. Lett.* **100**, 096407 (2008).

<sup>20</sup>J. Linder, Y. Tanaka, T. Yokoyama, A. Sudbø, and N. Nagaosa, *Phys. Rev. Lett.* **104**, 067001 (2010).

<sup>21</sup>M. Sato, Y. Takahashi, and S. Fujimoto, *Phys. Rev. Lett.* **103**, 020401 (2009).

<sup>22</sup>J. D. Sau and S. D. Sarma, *Nat. Commun.* **3**, 964 (2012).

<sup>23</sup>B. Braunecker, G. I. Japaridze, J. Klinovaja, and D. Loss, *Phys. Rev. B* **82**, 045127 (2010).

<sup>24</sup>T.-P. Choy, J. M. Edge, A. R. Akhmerov, and C. W. J. Beenakker, *Phys. Rev. B* **84**, 195442 (2011).

- <sup>25</sup>I. Martin and A. F. Morpurgo, *Phys. Rev. B* **85**, 144505 (2012).
- <sup>26</sup>S. Nadj-Perge, I. K. Drozdov, B. A. Bernevig, and A. Yazdani, *Phys. Rev. B* **88**, 020407 (2013).
- <sup>27</sup>Y.-M. Lu and Z. Wang, *Phys. Rev. Lett.* **110**, 096403 (2013).
- <sup>28</sup>H. Shiba, *Prog. Theor. Phys.* **40**, 435 (1968).
- <sup>29</sup>A. I. Rusinov, *Sov. Phys. JETP* **29**, 1101 (1969).
- <sup>30</sup>L. Yu, *Acta Phys. Sin.* **21**, 75 (1985).
- <sup>31</sup>A. Yazdani, B. A. Jones, C. P. Lutz, M. F. Crommie, and D. M. Eigler, *Science* **275**, 1767 (1997).
- <sup>32</sup>A. I. Buzdin, *Rev. Mod. Phys.* **77**, 935 (2005).
- <sup>33</sup>F. S. Bergeret, A. F. Volkov, and K. B. Efetov, *Rev. Mod. Phys.* **77**, 1321 (2005).
- <sup>34</sup>J. Linder, T. Yokoyama, and A. Sudbø, *Phys. Rev. B* **79**, 054523 (2009).
- <sup>35</sup>A. Fert, V. Cros, and J. Sampaio, *Nat. Nano.* **8**, 152 (2013).
- <sup>36</sup>S. Heinze, K. von Bergmann, M. Menzel, J. Brede, A. Kubetzka, R. Wiesendanger, G. Bihlmayer, and S. Blugel, *Nat. Phys.* **7**, 713 (2011).
- <sup>37</sup>See Supplemental Material at <http://link.aps.org/supplemental/10.1103/PhysRevB.88.180503> for more information.
- <sup>38</sup>A. V. Balatsky, I. Vekhter, and J.-X. Zhu, *Rev. Mod. Phys.* **78**, 373 (2006).
- <sup>39</sup>J. Hara and K. Nagai, *Prog. Theor. Phys.* **76**, 1237 (1986).
- <sup>40</sup>H.-J. Kwon, K. Sengupta, and V. M. Yakovenko, *Eur. Phys. J. B* **37**, 349 (2004).
- <sup>41</sup>S. Kashiwaya and Y. Tanaka, *Rep. Prog. Phys.* **63**, 1641 (2000).
- <sup>42</sup>M. Sato, Y. Tanaka, K. Yada, and T. Yokoyama, *Phys. Rev. B* **83**, 224511 (2011).
- <sup>43</sup>J. You, C. H. Oh, and V. Vedral, *Phys. Rev. B* **87**, 054501 (2013).
- <sup>44</sup>G. E. Volovik, *JETP Lett.* **70**, 609 (1999).
- <sup>45</sup>A. Furusaki, M. Matsumoto, and M. Sigrist, *Phys. Rev. B* **64**, 054514 (2001).
- <sup>46</sup>D. Asahi and N. Nagaosa, *Phys. Rev. B* **86**, 100504 (2012).
- <sup>47</sup>M. F. Crommie, C. P. Lutz, and D. M. Eigler, *Science* **262**, 218 (1993).
- <sup>48</sup>S. Fölsch, P. Hylgaard, R. Koch, and K. H. Ploog, *Phys. Rev. Lett.* **92**, 056803 (2004).
- <sup>49</sup>C. F. Hirjibehedin, C. P. Lutz, and A. J. Heinrich, *Science* **312**, 1021 (2006).
- <sup>50</sup>S. Loth, S. Baumann, C. P. Lutz, D. M. Eigler, and A. J. Heinrich, *Science* **335**, 196 (2012).